Angewandte Chemie
Eine Zeitschrift der Gesellschaft Deutscher Chemiker

Supporting Information

69451 Weinheim, Germany

Computed Tomography in Color: NanoK-Enhanced Spectral CT Molecular Imaging**

Dipanjan Pan, Ewald Roessl, Jens-Peter Schlomka, Shelton D. Caruthers, Angana Senpan, Mike J. Scott, John S. Allen, Huiying Zhang, Grace Hu, Patrick J. Gaffney, Eric T. Choi, Volker Rasche, Samuel A. Wickline, Roland Proksa, and Gregory M. Lanza**

anie_201005657_sm_miscellaneous_information.pdf
anie_201005657_sm_movie_1.avi
anie_201005657_sm_movie_2.avi

Concept of spectral CT

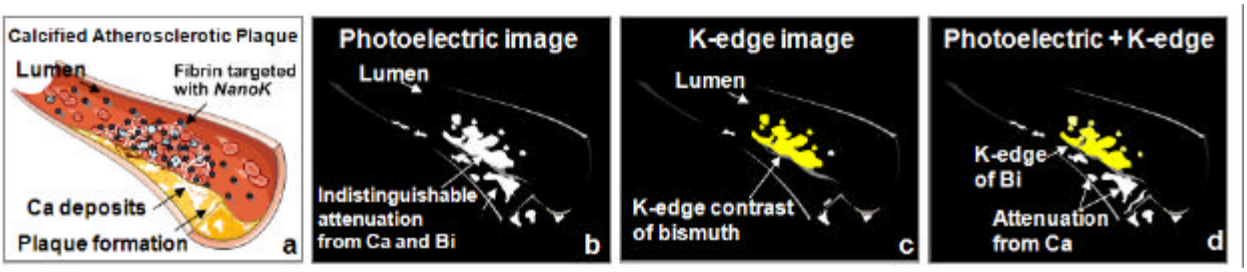

Figure 1. Illustration of the combined use of Spectral CT and fibrin-targeted NanoK (Bi) (e.g., bismuth) to characterize ruptured atherosclerotic plaque: (a) coronary artery with a partial occluding thrombus emerging from rupture of the unstable intimal cap, NanoK (Bi) targeted to thrombus fibrin; (b) in (classic CT) image with attenuation due to calcium and targeted NanoK (Bi) seen but indistinguishable; the thrombus is not apparent; (c) Spectral CT (K-edge imaging) detects the fibrin-targeted NanoK (Bi) but no other features; (d) integration of the simultaneous photoelectric (classic CT) and Spectral CT (K-edge) data provides a colorized map of thrombus superimposed on the traditional black and white CT image.

Stability of the nanocolloids

Preliminary long-term storage stability of the nanocolloids was assessed by measuring hydrodynamic diameter distributions over a period of >200 days from the time of synthesis for three replicate bismuth formulations preserved under inert atmosphere (i.e. argon) at 4°C. Changes in particle size and polydispersity indexes due to Ostwald ripening were minimal (< 10%) over the observation period (Supporting information Figure 2); phase microscopy revealed no evidence of particle aggregation or cracking.

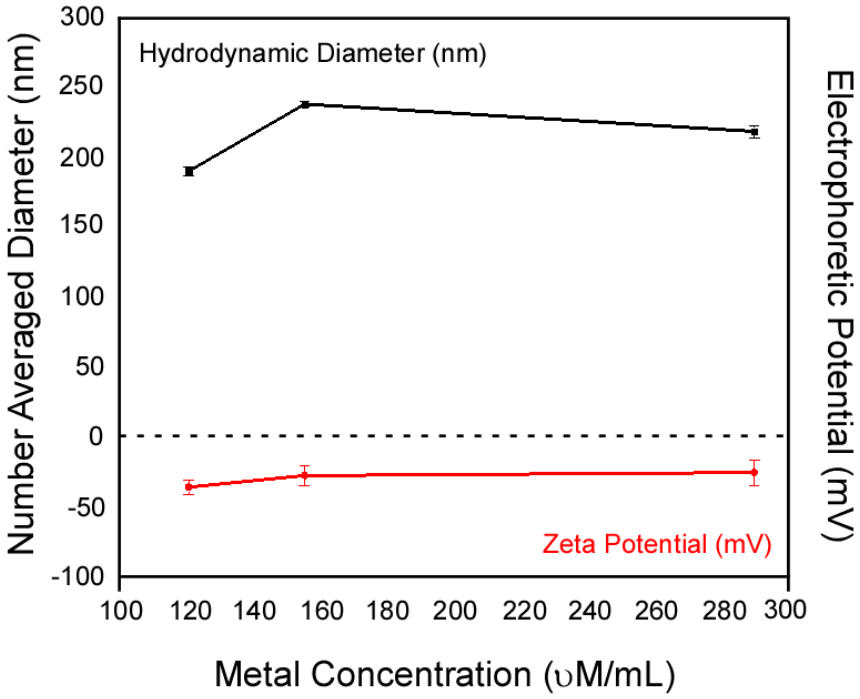

Figure 2(a). Number-averaged hydrodynamic diameter and electrophoretic potential values for NanoK replicates 1-3.

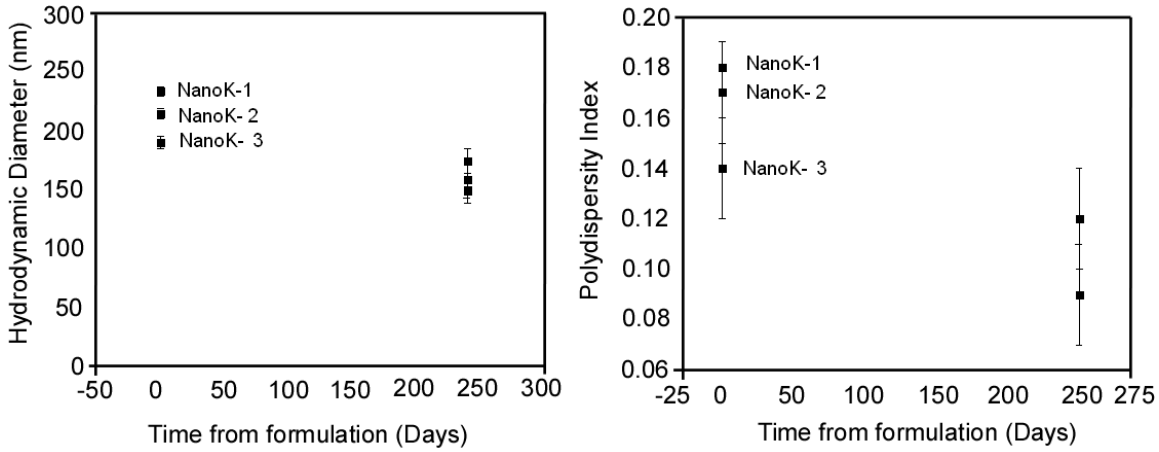

Figure 2b-c. Hydrodynamic diameters (Left) and polydispersity indexes (Right) of three replicates of NanoK, recorded immediately after formulation and after >eight months.

Blood smear experiment: Morphological changes in lymphocytes and blood clumping was observed in a blood smear preparation using clinical microscopy technique (conventional light microscopy) under high-

power field. Significant clumping or morphological changes were not observed in blood cells in animals treated with NanoK (blood: NP = 9:1) (Supporting information Figure 3)

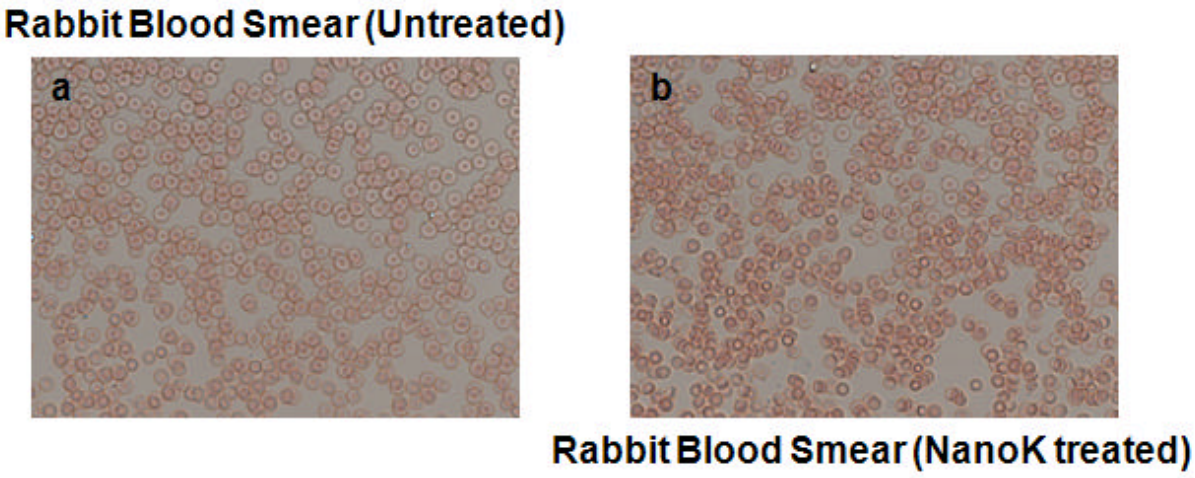

Figure 3. Optical microscopy images of blood smear untreated (a) and NanoK treated (b) (magnification: 40x).

Histology experiment

Frozen sections of CEA specimens exposed to rhodamine-labeled NanoK with (Figure 5a) and without fibrin-antibody (Figure 5c) demonstrated specific ligand mediated binding of NanoK to minute fibrin deposits layered along the luminal aspect of the tissue. Corresponding immunohistochemistry (Figures 5b, 5d, respectively) on adjacent frozen sections confirmed the surface presence of fibrin but also revealed deposits within the carotid plaque that were not enhanced by the lumen constrained fibrin-targeted NanoK particles.

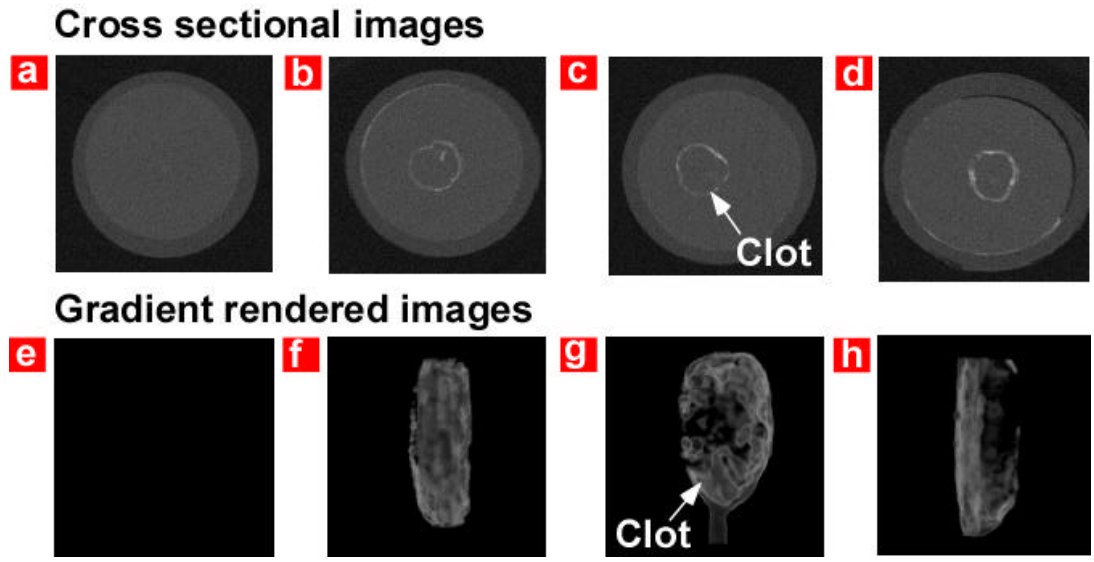

(i) (j)

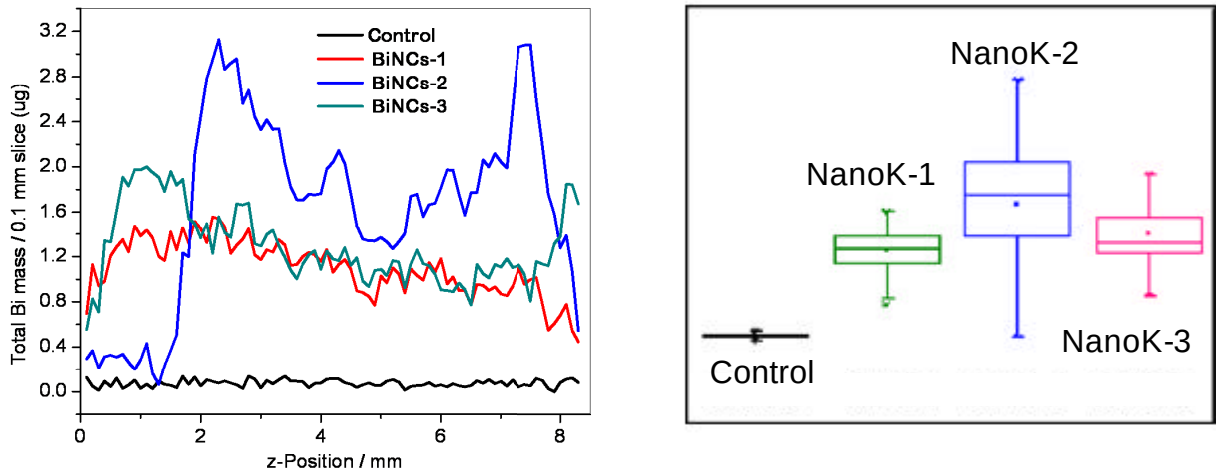

Figure 4. Spectral CT cross-sectional slices (Top) and gradient rendered images (Below) of fibrin clots targeted with control (a, e) and NanoK replicates (b-d, f-h); (Scale: 10 mm); (i-j) integral bismuth distribution in axial slices of fibrin clots: bound on bismuth layer thickness calculated with Scanner spatial resolution @ 100µm, voxel size in reconstructed image: $(100\mu m)^3$, bismuth layer thickness: 1-2 voxel; Bismuth surface density was calculated from integrations perpendicular to the surface layer corresponding to an average 3.5 mass% bismuth for a 100µm layer thickness.

Movies

Movie 1. Spectral CT movie of acellular fibrin clot targeted with NanoK.

Movie *2*. Spectral CT movie of human carotid specimen incubated with control nanocolloids (Right tube) and bismuth nanocolloids (Left tube) demonstrating bismuth signal resolve from intramural calcium deposits.

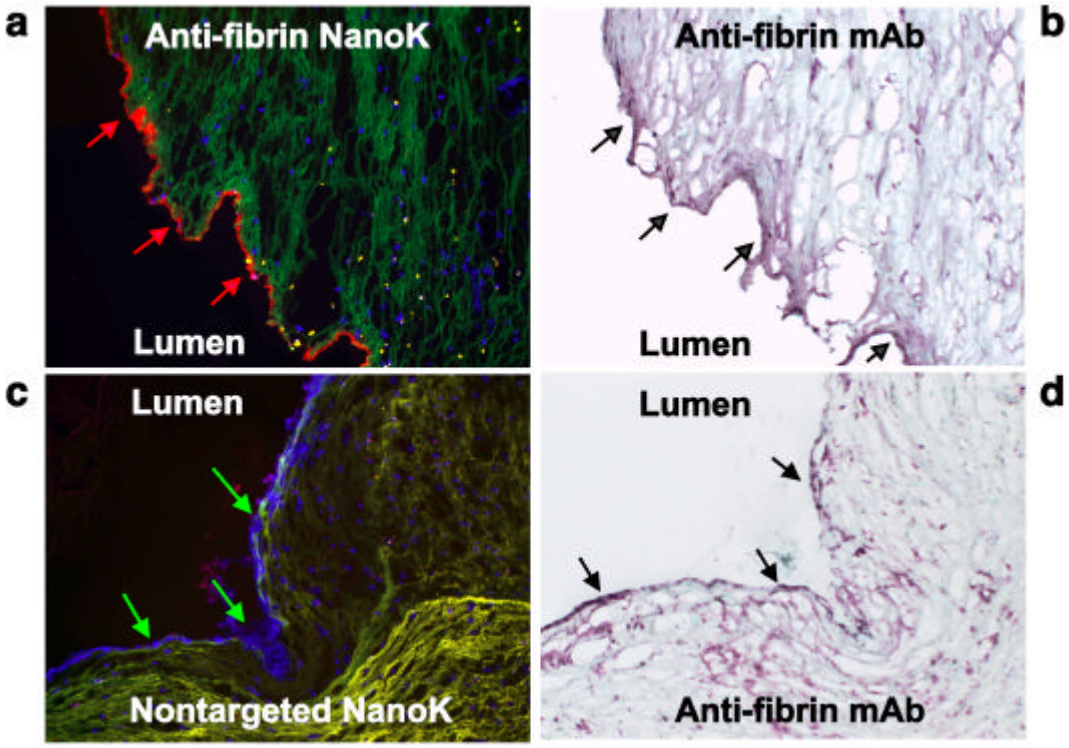

Figure 5. Frozen sections of CEA specimens exposed to rhodamine-labeled NanoK with (a) or without (c) fibrin-antibody targeting and counterstained with DAPI nuclear staining (blue). Immunostaining of adjacent sections confirm the presence of fibrin on the lumen surface, corresponding to NanoK rhodamine signal. Although fibrin was found by immunostaining within the plaque, no NanoK fluorescent signal was observed in the wall, reflecting the intravascular-constrained specificity advantage of the 200nm agent.

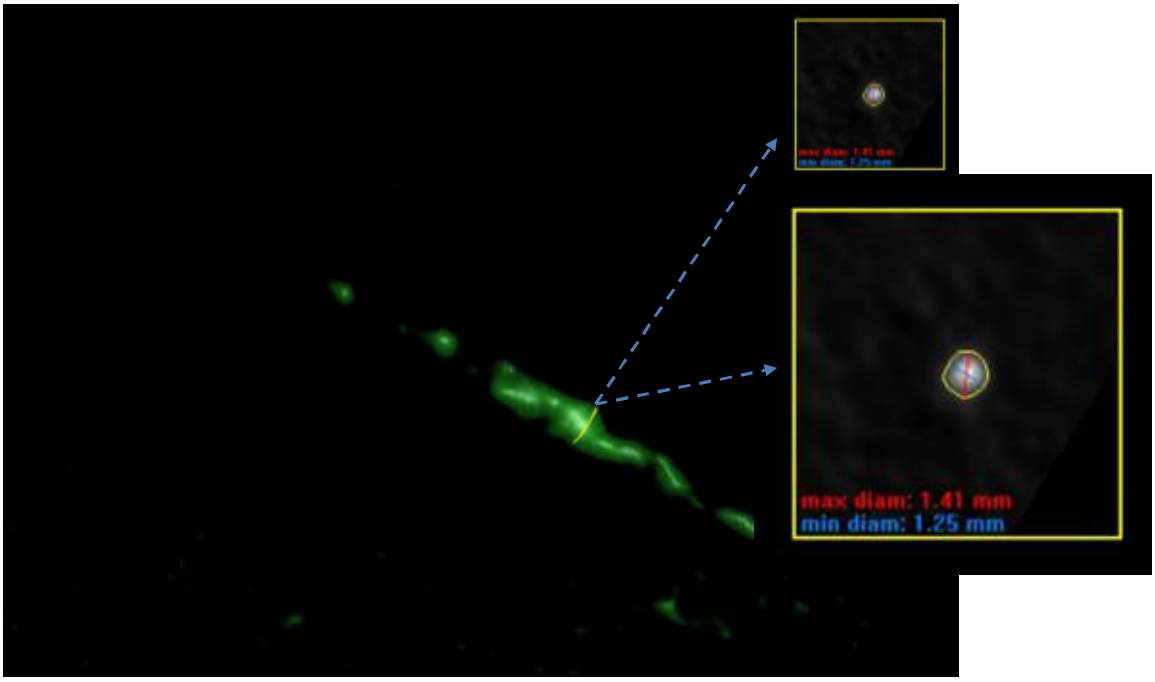

Figure 6. Measurements of the diameter of the clot: Maximum diameter: 1.41mm, Minimum diameter: 1.25mm.

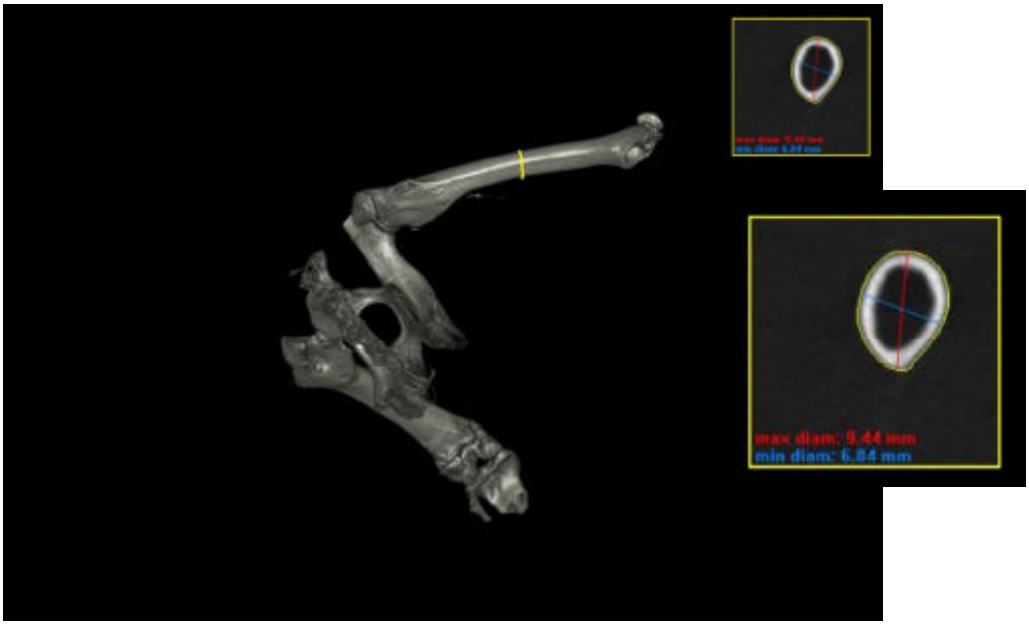

Figure 7. Measurements of the diameter of the bones.

Table 1. Safety evaluation of NanoK (Bi) by liver function tests

Test	Control (No treatment)	NanoK (Bi) treated Days		
		24h	7d	14d
Blood Urea Nitrogen (mg/dL)	17.0±2.0	20.7±3.1	25.3±2.1	16.3±2.1
Creatinine (mg/dL)	0.3±0.0	0.2±0.0	0.2±0.1	0.2±0.0
Albumin (g/dL)	2.6±0.0	1.9±0.2	2.0±0.0	1.8±0.1
AST (u/L)	126.3±40.5	101.7±42.2	102.7±34.7	102.3±28.9
ALT (u/L)	47.0±1.0	89.7±16.3	53.0±15.1	47.3±24.3
Potassium (K) (mmol/L)	5.7±0.6	5.9±0.6	5.2±0.5	4.4±0.4
Chloride (Cl) (mmol/L)	115.3±1.2	105.3±3.8	107.3±3.5	110.0±4.4
Sodium (Na) (mmol/L)	136.3±3.5	128.7±5.5	132.0±4.6	134.3±6.1

Methods

Unless otherwise listed, all solvents and reagents were purchased from Aldrich Chemical Co. (St. Louis, MO) and used as received. Anhydrous chloroform was purchased from Aldrich Chemical Co. and distilled over calcium hydride prior to use. Biotinylated dipalmitoyl-phosphatidylethanolamine and high purity egg yolk phosphatidylcholine were purchased from Avanti Polar Lipids, Inc. Cholesterol, bismuth neodecanoate and sorbitan sesquioleate were purchased and used as received from Aldrich Chemical Co. (St. Louis, MO). Argon and nitrogen (UHP, 99.99%) were used for storage of materials. The Spectra/Por membrane (Cellulose MWCO: 10 000 Da) used for dialysis was obtained from Spectrum Medical Industries, Inc. (Laguna Hills, CA).

Dynamic light scattering measurements

Hydrodynamic diameter distribution and distribution averages for the NanoK and controls in aqueous solutions were determined by dynamic light scattering. Hydrodynamic diameters were determined using a Brookhaven Instrument Co. (Holtsville, NY) Model Zeta Plus particle size analyzer. Measurements were made following dialysis (MWCO 10 kDa dialysis tubing, Spectrum Laboratories, Rancho Dominguez, CA) of NanoK suspensions into deionized water (0.2 mM). Nanoparticles were dialyzed into water prior to analysis. Scattered light was collected at a fixed angle of 90°. A photomultiplier aperture of 400 mm was used, and the incident laser power was adjusted to obtain a photon counting rate between 200 and 300 kcps. Only measurements for which the measured and calculated baselines of the intensity autocorrelation function agreed to within +0.1% were used to calculate nanoparticle hydrodynamic diameter values. All determinations were made in multiples of five consecutive measurements.

Electrophoretic potential measurements

Zeta potential (z) values for the NanoK were determined with a Brookhaven Instrument Co. (Holtsville, NY) model Zeta Plus zeta potential analyzer. Measurements were made following dialysis (MWCO 10 kDa dialysis tubing, Spectrum Laboratories, Rancho Dominguez, CA) of NanoK suspensions into water. Data were acquired in the phase analysis light scattering (PALS) mode following solution equilibration at 25°C. Calculation of z from the measured nanoparticle electrophoretic mobility (ζ) employed the

Smoluchowski equation: $\mu = \varepsilon\zeta/\eta$, where ε and η, are the dielectric constant and the absolute viscosity of the medium, respectively. Measurements of ζ were reproducible to within ±4 mV of the mean value given by 16 determinations of 10 data accumulations.

Inductively coupled plasma-optical emission spectroscopy

After imaging, the bismuth content of NanoK was analyzed by inductively coupled plasma-optical emission spectroscopy (ICP-MS, SOP7040, Rev 9) conducted at the Bodycote, West Coast Analytical Service (WCAS), Santa Fe Springs, CA. Briefly, the samples were analyzed by a Leeman Labs Direct Reading Echelle ICP-MS, or a DRE instrument which was designed to handle sub-ppm to percent level bismuth concentrations.

***In vitro* human plasma clot phantoms**

In a typical procedure, whole porcine blood was obtained fresh and anticoagulated (9:1, vol/vol) with sterile sodium citrate. Plasma clots were produced by combining plasma and 100 mmol/L calcium chloride (3:1 vol/vol) with 5 U thrombin (Sigma-Aldrich, Inc.) in a (low density polyethylene) tube (~1 cc volume, I.D. ~6 mm). The plasma was allowed to coagulate slowly at room temperature. The clots were incubated individually with 150 µg biotinylated antifibrin monoclonal antibody (NIB5F3)[1-4] in 10 ml PBS with 1% crystalline BSA (Sigma Chemical Co) for 2 hours. The antibody-treated clots were then incubated with excess avidin (50 µg/ml PBS) for 30 minutes, followed by biotinylated NanoK (30 µL/ml PBS) for 30 minutes. The control clots were treated similarly with control nanoparticle (30 µl/ml PBS).

Spectral CT Imaging

The spectral CT prototype scanner and data processing method employed in our studies has been previously reported[5-6] for imaging phantoms. Optimized parameters for the detection of bismuth with K-edge energy of 90.8 keV were determined by simulation: tube voltage was set to ~130kVp and the six tunable energy-thresholds were 25.0, 48.0, 55.0, 85.0, 91.0, 110.0 keV on all 1024 pixels of the CdTe detector array. The scanner was operated at high magnification (M=6); images were reconstructed on an isotropic grid of 100x100x100 mm^3. Clot phantoms were scanned at 10 mAs per slice; the human carotid

samples at 7.5 mAs per slice. The attenuation was decomposed into photo-effect, Compton-effect and bismuth.

Human carotid samples

Human carotid endarterectomy samples were obtained post-surgically from symptomatic patients and frozen until treatment. After being thawed, the carotid artery was rinsed with sterile saline to remove residual blood. The artery was incubated with 125 mg biotinylated anti-fibrin monoclonal antibody (NIB 1H10) overnight at 4°C, followed by 125 mg avidin for 1 hr at 37°C, and then 100 ml of the selected biotinylated nanoparticles for 1 hr at 37°C to complete the binding. All samples were rinsed three times with sterile saline after each incubation step to remove any unbound reactants. Following the last incubation step, the carotid specimens were immersed in agarose for shipment and imaging.

Bio-elimination study

Six mice received NanoK (1ml/kg) via intravenous catheter and two mice served as saline-only controls. Of the six treated mice, two mice were sacrificed 2 minutes after iv injection to establish the maximum whole body concentration of bismuth. Subsequently, two mice were sacrificed from the remaining four animals on days 7 and 14 post injection. Carcasses of all 8 animals were independently frozen, ground to tissue homogeneity, weighed, and the entire specimen was submitted for bismuth content analysis using ICP-MS. The analytical ICP bismuth measurements on day 1 corresponded closely with the empirical estimates based on dose given and animal weight (Figure 6e). Using the average of these bismuth values as the 100% baseline, 94.6% was entirely eliminated by day 7 and 96.4% was excreted on day 14. Bismuth was undetected (detection limit: 0.005 μg/g) in the control mice. No adverse effects were observed in these animals during the in-life phase of the study, which reflected the lack of free bismuth bioavailability from bismuth neodecanoate.

Histology

Human carotid endarterectomy specimens were thawed then serially incubated with anti-fibrin monoclonal antibody (NIB 1H10), avidin, and biotinylated rhodamine NanoK. Control CEAs were treated identically except the anti-fibrin antibody was excluded. Unbound reactants were removed

between each step. The tissues were embedded in O.C.T. media (Fisher Scientific), cryo sectioned (8 μm), and adjacent sections were either counterstained with DAPI for fluorescent microscopy or immunostained with anti-fibrin antibody (1H10) using routine technique and the Vectastain ABC kit (Vector Laboratories, Burlingame, CA). Microscopic imaging was performed with Olympus BX61 using a Color View II camera for light microscopy, F-View II B&W CCD camera for fluorescent images, MicroSuite biological suite software for microscope control and image processing (Olympus America, Inc., Center Valley, PA).

Statistics

Spectral CT bismuth concentration data were analyzed using ANOVA procedure provided by SAS (SAS, Inc, Cary, NC) using a $p<0.05$ statistical threshold of significance.

References

1. Lanza GM, et al. A novel site-targeted ultrasonic contrast agent with broad biomedical application. Circulation **94**, 3334-3340 (1996).

2. Flacke S, et al. A novel MRI contrast agent for molecular imaging of fibrin: Implications for detecting vulnerable plaques. *Circulation* **104**, 1280-1285 (2001).

3. Lanza GM, et al. Enhanced detection of thrombi with a novel fibrin targeted magnetic resonance imaging agent. *Acad. Radiol.* **5** (Suppl 1), S173-S176, (1998).

4. Botnar RM, et al. *In vivo* magnetic resonance imaging of coronary thrombosis using a fibrin-binding molecular magnetic resonance contrast agent. *Circulation* **110**, 1463-1466, (2004).

5. Feuerlein S., et al. Multi energy Photon-counting K-edge Imaging: Potential for Improved Luminal Depiction in Vascular Imaging. Radiology 249, 1010-1016 (2008).

6. Schlomka, J. P., et al. Experimental feasibility of multi-energy photon-counting K-edge imaging in pre-clinical computed tomography. *Phys. Med. Biol.* **53**(15), 4031-4047 (2008).